ACS Photonics

Open Access

pubs.acs.org/journal/apchd5

Article

Polariton-Induced Transparency in Multiple Quantum Wells Probed by Time Domain Brillouin Scattering

Marek Karzel, Anton K. Samusev, Tetiana L. Linnik, Mario Littmann, Dirk Reuter, Manfred Bayer, Alexey V. Scherbakov,* and Andrey V. Akimov*

Cite This: https://doi.org/10.1021/acsphotonics.4c01357

Read Online

ACCESS | Metrics & More | Article Recommendations | Supporting Information

ABSTRACT: The interference of the incident light reflected from the surface of a medium and from a picosecond strain pulse propagating through it results in temporal oscillations of the reflected intensity. This phenomenon, called time-domain Brillouin scattering, enables us to gain information about the optical field inside the medium. The oscillation amplitude decreases with increase of the distance from the strain pulse to the surface if the incident light is strongly absorbed, while it remains constant if the medium is transparent. Here we exploit time domain Brillouin scattering to probe the optical field inside a multiple quantum well layer for light strongly coupling to excitons and forming polaritons. At low excitation density, we observe conventional Brillouin oscillations whose amplitude is small when the strain pulse is positioned far from the surface due to the strong absorption of polaritons in the vicinity of the exciton resonance. At elevated optical density, the absorption disappears, the medium becomes transparent, and the amplitude of the oscillations does not depend on the distance of the strain pulse from the surface. We explain this effect of polariton-induced transparency by the increase of the incoherent exciton density generated as result of polariton scattering. Finally, the increase of the exciton density leads to transition of the exciton gas to a collective state, resulting in collapse of the polariton state and propagation of the incident light in the medium without absorption.

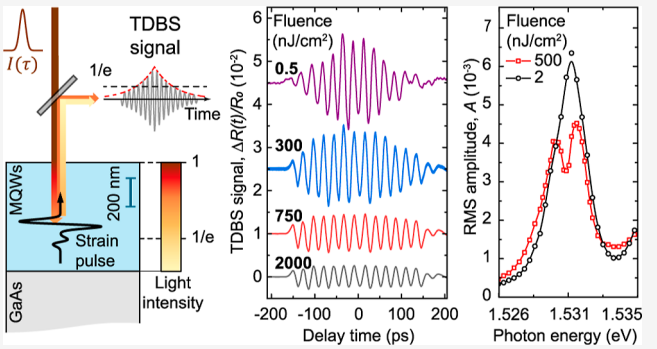

KEYWORDS: *polaritons, multiple quantum wells, picosecond ultrasonics, Brillouin scattering*

INTRODUCTION

The propagation of high-intensity optical pulses in a medium with an optical resonance leads to a number of nonlinear phenomena among which is the initially strongly absorbing medium becoming transparent.[1,2] There are several well-known coherent and noncoherent mechanisms responsible for such optically induced transparency. Among them are the phenomena of self-induced transparency[3,4] and saturable absorption,[5] discovered 50 years ago and intensively studied until today.[6−8] Optically induced transparency is widely used nowadays in laser technology for optical pulse shaping and compression,[9] for the generation of optical solitons,[10] and for slow light effects.[11−13] Typical experiments for studying optically induced transparency include measurements of the intensity and temporal shape of the light transmitted through a dispersive medium. With such an experimental approach, important information about the optical field and resonant excitation inside the medium remains masked and may be predicted only theoretically. Probing of the optical field inside the resonant medium is a challenging task that requires development of advanced experimental methods.

Here, we report experiments on optically induced transparency in a multilayer nanostructure with an optically active exciton resonance by probing the optical field inside the nanostructure with picosecond strain pulses and detecting the time domain Brillouin scattering (TDBS).[14−16] TDBS is the phenomenon where the electromagnetic wave reflected from the surface of the sample interferes with the wave reflected from the strain pulse propagating in the sample with sound velocity, s, toward the surface or away from it. The distance x between the strain pulse and the surface changes linearly with time leading to alternating conditions for destructive and constructive interference. As a result, the changes in the reflected light intensity $\Delta R(t)$ possess oscillations in time, as shown in Figure 1a, which demonstrates the typical experimental scheme for studying TDBS. Generally, the

Received: July 22, 2024
Revised: November 23, 2024
Accepted: November 25, 2024

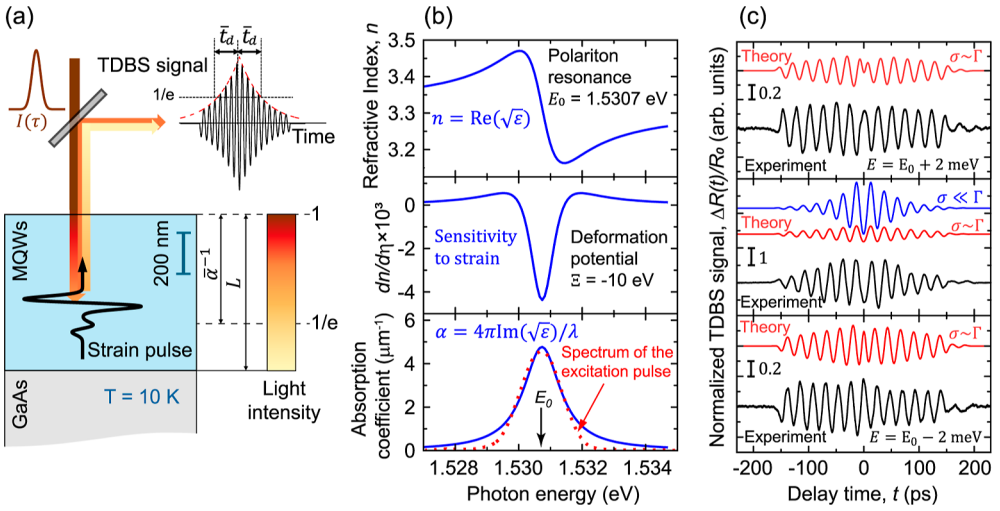

Figure 1. (a) Scheme of the experiment for measuring TDBS signals. (b) Main polaritonic properties of the GaAs/AlGaAs MQWs in vicinity of the exciton resonance as a function of photon energy E: (upper panel) refractive index $n(E)$; (middle panel) reduced photoelastic constant determining the sensitivity to strain; (lower panel) absorption coefficient for intensity $\alpha(E)$; the dashed line in the lower panel is the Gaussian intensity spectrum of the excitation pulse when its center corresponds to the exciton resonance at $E = E_0$. (c) Measured (black lines) and simulated (red lines) TDBS signals for low fluence excitation at the center ($E = E_0$, middle panel) and wings (upper and lower panels) of the exciton resonance; blue line in the middle panel is calculated TDBS signal when the spectral width of excitation is much smaller than the width of the exciton resonance. For relative amplitudes see vertical bars.

waveform $\Delta R(t)/R_0$ (R_0-the reflected intensity without the strain pulse) of these oscillations may be described as

$$\Delta R(t)/R_0 = C(t)\sin(2\pi f_B t + \varphi) \quad (1)$$

where the Brillouin frequency f_B, the phase φ and the envelope function $C(t)$ are governed by the dielectric properties of the medium and the spatial shape profile of the propagating strain pulse $\eta(x - st)$.[14−16] For the experimental scheme shown in Figure 1a, $C(t)$ is close to a symmetric function with respect to $t = 0$, i.e., the time when the strain pulse hits the surface. The time intervals $t < 0$ and $t > 0$ correspond to the strain pulse propagating toward the surface and backward away from it (after reflection at the surface), respectively. In the simplest case of a homogeneous medium where the permittivity of the medium ε does not depend on x and t and also, when the permittivity is almost constant in the spectral range of the incident light, $C(|t|)$ is an exponentially decaying function with the time constant $t_d = (\alpha s)^{-1}$, where α is the optical absorption coefficient: $\alpha = 4\pi\kappa/\lambda$ ($\kappa = \mathrm{Im}\{\sqrt{\varepsilon}\}$ and λ is the optical wavelength). In this case the oscillation frequency[14−16]

$$f_B = 2sn/\lambda \quad (2)$$

where $n = \mathrm{Re}\{\sqrt{\varepsilon}\}$.

The waveform $C(t)$ of the TDBS signal becomes more complicated if ε is a function of time t and distance x. Moreover, if the optical wave is not monochromatic, the dispersion of the medium $\varepsilon(E)$ (E is the photon energy) becomes important.[17] Then, the resulting waveform of the TDBS signal governed by these dependencies allows us to get information about the optical field and, finally, about the complex dielectric properties inside the medium. Nowadays, TDBS and related experimental techniques are widely used to probe internal interfaces,[18,19] buried defects,[20] the speed of chemical reactions[21] and the optical field in multilayers[22] with nanometer depth resolution. In the present work, we exploit TDBS signals to extract information about the optical field inside a multilayer nanostructure in the nonlinear regime when optically induced transparency is dominant.

RESULTS AND DISCUSSION

In the experiments performed at $T = 10$ K we use GaAs/(Al,Ga)As multiple quantum wells (MQWs) with the exciton resonance at $E_0 = 1.5307$ eV. In the MQWs, light with photon energy E in the vicinity of the exciton resonance is converted to a polariton which is an electromagnetic wave coherently coupled to the exciton resonance.[23,24] The term "polariton" was introduced in 1958 for bulk semiconductors in the pioneering work of Hopfield[25] and in MQWs using this term is valid as long as the dispersion of electromagnetic wave differs from being linear. Polaritons in MQWs have been studied in detail in high-resolution Brillouin scattering experiments.[26−28] For light incident normal to the plane of short period MQWs, the system may be described as a bulk medium with the effective permittivity ε[23,24,26−28]

$$\varepsilon(E) = \varepsilon_b\left[1 + \frac{E_{LT}}{E_0 - E - i\Gamma}\right] \quad (3)$$

In our sample the background dielectric constant $\varepsilon_b = 11.2$, the longitudinal-transverse splitting $E_{LT} = 0.13$ meV and for low excitation density the nonradiative dephasing rate $\Gamma = \Gamma_0 = 0.7$ meV are obtained from measurements of reflectivity spectra. The MQWs are excited by the optical pulses from a femtosecond laser after passing the beam through a tunable narrowband optical filter whose central wavelength is varied in the vicinity of the polariton resonance (see Methods). The duration of the excitation pulse for the intensity is $\tau_e = 1.1$ ps at the level $1/\sqrt{e}$. The polaritonic features of the studied MQW are clearly seen in the dependence of TDBS frequency on the excitation wavelength.[17]

The strain pulses $\eta(x)$ are generated by 100 fs laser pulses exciting a 100 nm thick Al film deposited on the surface opposite to the MQWs layer. The spatial profile of the strain pulse shown in Figure 1a is taken from earlier studies reported

https://doi.org/10.1021/acsphotonics.4c01357
ACS Photonics XXXX, XXX, XXX−XXX

elsewhere.[29] We present the experimental and theoretical results for the excitation density of 60 μJ/cm^2 on the Al film. This corresponds to the estimated strain pulse amplitude of $\sim 5 \times 10^{-6}$, the spatial width between the main positive and negative strain peaks in the pulse is ~50 nm. However, at low temperatures T there is an uncertainty in estimating the exact values for amplitude and duration of the strain pulse (see Methods and Supporting Information S2). The pulse is propagating through the GaAs layer and further the MQWs structure with longitudinal sound velocity (in the MQWs s = 5.04 km s^{-1}). In the experiments, we measure the relative changes of the reflectivity $\Delta R(t)/R_0$ as a function of the delay time t, which defines the position of the strain pulse when the picosecond laser pulse excites the MQWs. We define $t = 0$ as the moment when the center of the strain pulse reaches the surface. Correspondingly, the strain pulse is propagating toward this surface for $t < 0$ and back from the surface toward the substrate after reflection for $t > 0$. The measurement time t is controlled in experiment by a variable delay line in the path of the optical pulses that excite the Al film.

The dielectric properties of the MQWs which govern the TDBS signal for linear optical response (i.e., low fluence) are presented in Figure 1b. The upper panel in Figure 1b shows the real part of the refractive index $n(E) = \mathrm{Re}\{\sqrt{\varepsilon(E)}\}$ which has the typical shape for a system with a two-level optical resonance. The middle panel in Figure 1b shows the reduced photoelastic constant $dn(E)/d\eta$ which governs the reflectivity of the polaritons due to the strain pulse and correspondingly determines the amplitude of the TDBS signal.[30] This dependence shows a negative peak at the photon energy matching the energy of the exciton resonance at $E = E_0$ with a value governed by the deformation potential in GaAs $\Xi = dE_0/d\eta = -10$ eV.[31] The solid line in the lower panel of Figure 1b shows the absorption coefficient $\alpha(E)$ calculated from eq 3. The dashed line in the lower panel in Figure 1b is an example of the measured spectrum of the excitation pulse with the central wavelength corresponding to the energy of the exciton resonance E_0. The spectrum fits well with a Gaussian profile with the spectral width σ = 1.3 meV on the level $1/\sqrt{e}$. The dependences shown in Figure 1b govern the main features of the TDBS oscillations given by eq 1.

The black lines in Figure 1c show the TDBS signals measured at low excitation fluence J = 100 nJ/cm^2 for three excitation wavelengths λ. This value of J corresponds to the linear excitation regime when the dielectric properties of the MQWs are not affected by the pulse, and the temporal profiles $\Delta R(t)/R_0$ do not depend on the excitation fluence for fixed E. The TDBS signals last from $t = -160$ ps up to $t = 160$ ps which is close to twice the time of strain pulse propagation across the MQW structure $2L/s$ = 310 ps. The middle panel corresponds to the signal measured at the exciton resonance $E = E_0$ and the two other ones show the signals measured when E is located in the higher or lower spectral wings of the exciton resonance. All signals show typical TDBS oscillations with the frequency $f_B \sim$ 42 GHz which varies slightly with the excitation wavelength following the dependence of n on E (see eq 2 and upper panel in Figure 1b). The fast Fourier spectrum of TDBS signals also show high-frequency lines due to folded acoustic phonons in the MQWs.[17] In our experimental scheme and studied MQWs the intensity of these spectral lines are ~100-times smaller than at $f = f_B$ due to the relatively long strain pulse and will not be considered further in the present work. In agreement with the dependences of the sensitivity to strain (middle panel in Figure 1b), the $\Delta R(t)/R_0$ measured at $E = E_0$ demonstrates the maximum amplitude around the turning point ($t = 0$) compared to the signals measured at $E = E_0 \pm 2$ meV (note the different scales in the panels). In the general case, the envelope function $C(t)$ of the TDBS signal is not exponential because the spectral width σ of optical excitation is not much smaller than the width $\sim 2\Gamma_0$ of the exciton resonance. However, we may describe the decay of $C(|t|)$ by the mean decay time $\bar{t}_d$ measured when $C(t)$ reaches the $1/e$ level and then bring into consideration the effective absorption coefficient $\bar{\alpha} = (\bar{t}_d s)^{-1}$. From the measured signals presented in Figure 1c we get $\bar{\alpha} \sim 2\ \mu\mathrm{m}^{-1}$ at $E = E_0$ and smaller values $\bar{\alpha} \ll 1/L$ at the wings of the exciton resonance. Such relation between $\bar{\alpha}$ at the resonance and the wings is consistent with the absorption $\alpha(E)$ being larger at $E = E_0$ (see the lower panel in Figure 1b).

The red curves in Figure 1c are the $\Delta R(t)/R_0$ calculated using the transfer matrix method taking into account the Gaussian spectrum of excitation. Good agreement between the temporal shapes of the measured and simulated dependences $\Delta R(t)/R_0$ is clearly seen by comparing the red and black curves in Figure 1c. The amplitudes of the measured and calculated signals are of the same order of magnitude. The amplitude in the calculated signals is approximately half that of the measured signals which can be explained by the uncertainty in strain pulse shape and amplitude. We also present the results of a simplified model calculation assuming long monochromatic excitation pulse ($\sigma \ll \Gamma$). The signal calculated with this assumption for $E = E_0$ is shown by the blue line in the middle panel. It is seen that such simplification leads to an increase of the amplitude at $t \sim 0$ and a decrease of the mean decay time down to $\bar{t}_d \sim 47$ ps. In this case, the agreement with the experimentally measured $\Delta R(\Delta t)/R_0$ is not as good as for the Gaussian excitation pulse, but qualitatively the simulated signals show the same features such as maximum amplitude at $t \sim 0$ and short decay time $\bar{t}_d$ when $E = E_0$. At the spectral wings the differences between the results of the simplified approach ($\sigma \ll \Gamma$, not shown in Figure 1c) and the Gaussian excitation pulse ($\sigma \sim \Gamma$) are not significant. For a more detailed theoretical modeling of the TDBS signals detected in the MQW layer at low excitation fluence we refer to earlier studies.[17]

Now we turn to the main results of the present work which concern the TDBS signals measured at elevated fluences J. Figure 2 presents the results for resonant excitation $E = E_0$. The signals $\Delta R(t)/R_0$ measured for four values of J from J = 0.5 nJ/cm^2 up to J = 2000 nJ/cm^2 are shown in Figure 2a. At the lowest fluence $\Delta R(t)/R_0$ (see the topmost curve in Figure 2a) demonstrates the typical features of a TDBS signal described when presenting the results for the linear regime in Figure 1c. For J = 300 nJ/cm^2 the mean decay time of the oscillation amplitude becomes longer with $\bar{t}_d$ = 166 ps and the amplitude of the oscillations at $t \sim 0$ decreases. The increase of J to 750 nJ/cm^2 and further up to 2000 nJ/cm^2 results in signals $\Delta R(t)/R_0$ without any visible amplitude decay ($\bar{t}_d > 1$ ns) and to dropping of the amplitude around $t \sim 0$ to value of about 20% relative to the amplitudes measured for J < 250 nJ/cm^2. This experimental result allows us to draw the main conclusion of the present work: the mean decay time $\bar{t}_d$ of the TDBS oscillations increases with increasing J which corresponds to a decrease of the effective absorption

https://doi.org/10.1021/acsphotonics.4c01357
ACS Photonics XXXX, XXX, XXX−XXX

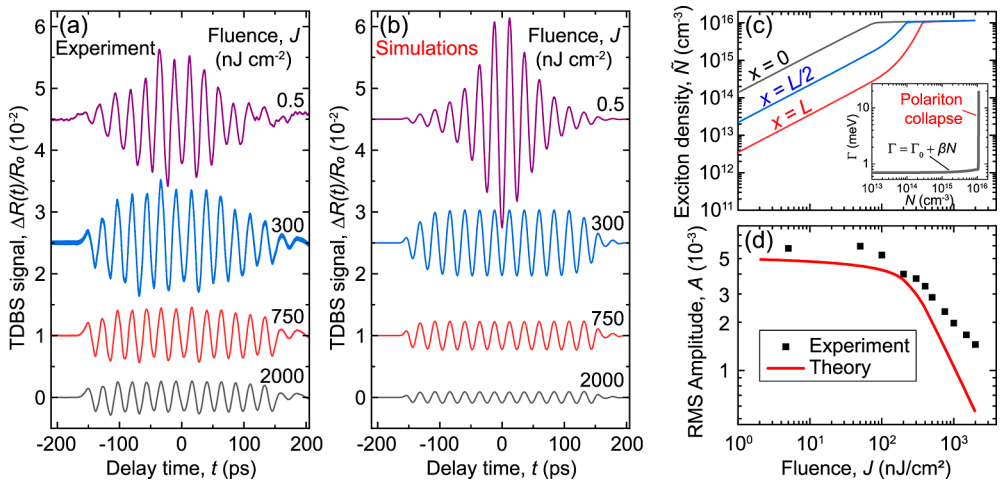

Figure 2. Measured (a) and simulated (b) TDBS signals for resonant excitation $E = E_0$ and various fluences J. (c) Calculated dependences of the exciton quasi-stationary density $\tilde{N}$ at time $\tilde{\tau}$ after the excitation pulse ($\tau_e \ll \tilde{\tau} \ll \tau_a$) on the excitation fluence J for three distances x from the surface of the MQW layer; the inset shows the model dependence of Γ on the exciton density N (see eq 4). (d) Measured (squares) and calculated (solid line) dependences of the root-mean-square (RMS) amplitude of the TDBS signal on the excitation fluence.

coefficient $\bar{\alpha}$ when exciting at the exciton resonance $E = E_0$. This has to be interpreted as experimental demonstration of polariton-induced transparency, a conclusion that needs to be validated by a model that explains the transformation of absorption and other dielectric properties of the studied MQW structure at high fluence.

The basis for our phenomenological model is the nonradiative scattering of the polaritons described by the dephasing rate Γ (see eq 3) which at low exciton density and low temperature ($\Gamma = \Gamma_0$) is governed by various defects and inhomogeneities in the MQWs.[32] Actually Γ may include contribution from the inhomogeneous broadening of the exciton resonance but this does not change significantly the dependences in Figure 1b and TDBS signals in Figure 1c (see also Supporting Information S5). As result of the dephasing, energy is transferred to incoherent excitons which have a lifetime of $\tau_a \sim 1$ ns.[33] It is well-known that in quantum wells, Γ increases with increase of the exciton density N[34−40] and at some threshold exciton density $N_t \sim 10^{16}$ to 10^{17} cm^{-3}, the exciton gas undergoes the Mott transition and further the transition to an electron−hole plasma.[36−40] For $N > N_t$, the MQW layer stops behaving as a resonant two-level system and the propagating polariton transforms into a conventional optical wave propagating in a nondispersive medium with $\varepsilon \sim \varepsilon_b$. In the simulations, we model the dependence of Γ on exciton density N as a linear function[34,35] at low N and as rapid exciton damping when N approaches the threshold value N_t

$$\Gamma = \Gamma_0 + \beta N + \mathcal{R}(N - N_t, \Delta N) \tag{4}$$

where the phenomenological function $\mathcal{R}$ describes the exciton gas phase transition and collapse of the polaritons at $N > N_t$ (for details see Methods). The value of ΔN characterizes the width of the phase transition. Further, we present the results of modeling for $N_t = 10^{16}$ cm^{-3}. We assume that the phase transition has a very abrupt threshold, $\Delta N = 2 \times 10^{14}$ cm^{-3}, which is in agreement with THz experiments.[39] It will be shown that the coefficient β is not very important for qualitative conclusions, but based on earlier studies[34,35] we cannot ignore the linear part in eq 4 and take $\beta = 10^{-17}$ meV/cm^3. The model dependence of Γ on N is shown in the inset of Figure 2c.

In the model, it is essential to consider the temporal evolution of the optical Gaussian excitation pulse $I(\tau)$ with the duration $\tau_e \sim 1$ ps. Then the density of generated excitons $N(x,\tau)$ and, correspondingly, polariton dephasing rate are dependent on the distance from the surface x and time τ. It is worth mentioning that the time τ is the momentary time of the excitation pulse $I(\tau)$ and is different from the delay time t, which defines the spatial position of the strain pulse in the MQWs. During excitation, the incoherent exciton density $N(x,\tau)$ increases and at time $\tau = \tilde{\tau}$ after the excitation pulse ($\tau_e \ll \tilde{\tau} \ll \tau_a$) it reaches the quasi-stationary level $\tilde{N}(x)$. At low J, when nonlinear effects are not important, we have

$$\tilde{N}(x) = (1 - R_0)\left(J\alpha/eE\right)e^{-\alpha x} \tag{5}$$

where E is taken in eV and R_0 is the reflectivity of the incident beam. At high fluence, when $\Gamma(x,\tau)$ and correspondingly $\varepsilon(x,\tau)$ (see eq 3) depend on τ and x, the dependence of $\tilde{N}$ on J becomes nonlinear. The details of our calculations are presented in Methods and Supporting Information S1. The main assumption of the simulations is that the scattering of polaritons to incoherent excitons happens immediately. We also do not account for the spectral width of the optical excitation. These assumptions, which allow for reasonably time-efficient calculations, do not guarantee good quantitative agreement with the experiment, but we believe that the model adequately describes the nonlinear effects on a qualitative level.

The calculated dependences of $\tilde{N}$ on J near the surface ($x = 0$), in the middle ($x = L/2$) and at the inner edge ($x = L = 778$ nm) of the MQW layer are presented in Figure 2c. The ratio $\frac{\tilde{N}(x=L)}{\tilde{N}(x=0)} < 1$ reflects the effective absorption $\bar{\alpha}$ of polaritons while they are propagating through the MQWs layer. It is seen that in the linear regime, when $J \leq 100$ nJ/cm^2, $\alpha = 4.4$ μm^{-1} which corresponds to a quite strong polariton absorption. For higher J the absorption decreases, $\tilde{N}(x)$ possesses a nonlinear dependence on J, and finally at $J = 400$ nJ/cm^2, $\tilde{N}(x)$ becomes almost homogeneous and saturates at a level $\sim N_t$ along the whole MQWs layer. This behavior confirms that the used model qualitatively describes the effect of polariton-induced transparency.

https://doi.org/10.1021/acsphotonics.4c01357
ACS Photonics XXXX, XXX, XXX−XXX

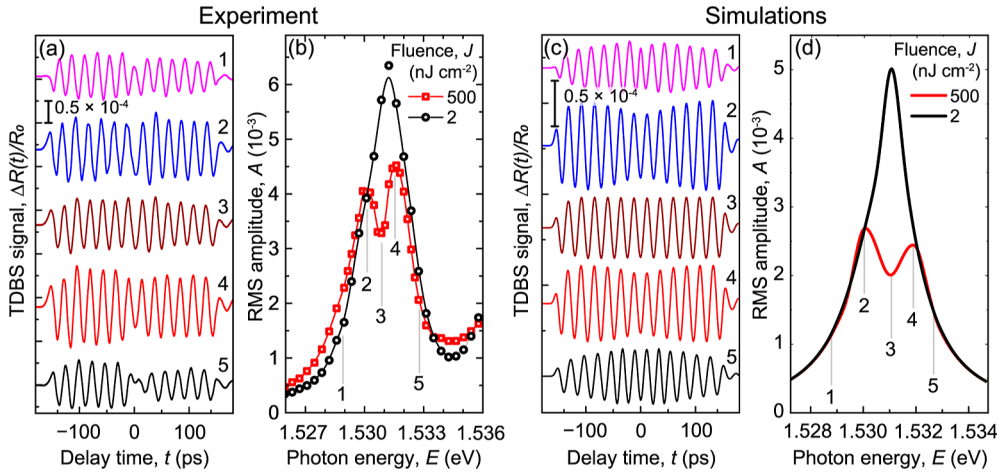

Figure 3. Measured (a) and calculated (c) TDBS signals for various photon energies E around the exciton resonance. The values of E are indicated by the vertical bars in (b,d) where the measured and calculated dependencies of the RMS amplitude of the TDBS signal on photon excitation energy are shown for high (J = 500 nJ/cm^2) and low (J = 2 nJ/cm^2) excitation fluences. Lines, which connect the symbols in (b), are guides for the eye.

For modeling the TDBS signals, we use a transfer matrix formalism substituting the calculated dependence of $\varepsilon(x,\tau)$ for each J. The simulated results for several J and $E = E_0$ are shown in Figure 2b. Comparing the experimental and simulated TDBS oscillations (Figure 2a,b respectively), we find that there is good qualitative agreement in the dependence of the decay rate $\overline{t}_d$ and correspondingly $\overline{\alpha}$: for low J the oscillations are clearly decaying with the increase of $|t|$ while at high J this decay is hardly seen due to optically induced transparency.

In parallel with the decrease of absorption we observe the decrease of the oscillation amplitude with increasing J. For the analysis, we use the root-mean-square (RMS) amplitude $A = \sqrt{\frac{1}{t_2 - t_1}\int_{t_1}^{t_2}[\Delta R(t)/R_0]^2 \mathrm{d}(t)}$, ($t_2 = -t_1 = 200$ ps). The experimental and calculated dependences $A(J_0)$ are shown in Figure 2d. At low fluence, A is almost independent of J while at $J > 100$ nJ/cm^2, a decrease of A with increasing J takes place. The decrease of A starts at approximately the same fluences for the measured and simulated signals. The disagreement in the absolute values of A is due to the model simplifications described above. Qualitatively the decrease of A with increasing J is consistent with the model where Γ increases with J. Indeed, the increase of Γ leads to broadening of the exciton resonance and decreasing of the sensitivity at $E = E_0$ (see the middle panel in Figure 1b).

Now we turn to the dependences of the TDBS signals on the photon excitation energy E in the nonlinear regime (J = 500 nJ/cm^2), presented in Figure 3. Five signals are shown for selected values of E, indicated by the vertical bars in Figure 3b,d. The TDBS oscillations in the experimental (Figure 3a) and theoretical (Figure 3c) signals 2, 3, and 4 do not show significant changes in the amplitude with t, which means that the absorption is small due to polariton-induced transparency in the MQWs. The theoretical signals 2 and 4 show an unusual increase of the oscillation amplitude with the increasing $|t|$. This behavior indicates that the sensitivity to strain $\mathrm{d}n(x,\tau)/\mathrm{d}\eta$ increases with x (it is higher in the depth of the MQW layer than at its open surface), in accordance with our model. At the spectral wings, signals 1 and 5 do not differ much from the case of the linear regime because there the absorption is already low at low power.

Figure 3b,d show the experimental and simulated dependences, respectively, of the RMS amplitude, A, on the photon energy E. The black circles (Figure 3b) and corresponding line (Figure 3d) show $A(E)$ for the low J = 2 nJ/cm^2, corresponding to the linear regime. The red squares (Figure 3b) and corresponding line (Figure 3d) demonstrate $A(E)$ for J = 500 nJ/cm^2 when the polariton-induced transparency has gained full strength. The striking difference between $A(E)$ at low and high fluences is observed at $E \sim E_0$. At low fluence, the spectral profile $A(E)$ behaves conventionally following the dependence of $\mathrm{d}n(E)/\mathrm{d}\eta$ on E (see Figure 1b) with the maximum at $E = E_0$ in a full agreement with earlier studies.[17] At high fluence, there is a dip at $E = E_0$ while the maxima of A are observed shifted by ±0.7 and 0.8 meV in the measured and simulated dependences, respectively. Varying the parameters in eq 5 we show that the dip can be simulated only when taking into account the abrupt exciton phase transition at $N \sim N_t$. Any power function of Γ on N leads only to a decrease of A without a dip at $E = E_0$. Qualitatively there is a balance between the depth dependent absorption of polaritons and their survival in MQWs which provides the resulting amplitude of TDBS signal. It is clear that the fluence threshold is reached earlier for the excitation at the exciton resonance which leads to the strong decrease of the sensitivity to strain relatively to the case when exciting at the wings of the resonance. For the dependence of $A(E)$ calculated for various parameters we refer to Section S4 in the Supporting Information.

The results presented in Figures 2 and 3 clearly show how TDBS probes the effect of polariton-induced transparency at high fluence. The decisive physical reason for the observed phenomenon is the exciton phase transition and corresponding collapse of the polaritons at high fluence. The phenomenological model used in our work unambiguously demonstrates the effect of polariton-induced transparency at high fluence, and highlights the fundamental physics processes responsible for the observed phenomenon. The simplifications of our model do not allow us to get the exact quantities like the threshold fluence for exciton phase transition, width of the phase transition, and amplitude of TDBS signal. However, the model allows us to make the qualitative conclusion about the

https://doi.org/10.1021/acsphotonics.4c01357
ACS Photonics XXXX, XXX, XXX−XXX

decisive role of the exciton phase transition in the observation of optically induced transparency.

Finally, we reveal a new effect of optically induced transparency in a resonant medium with polaritons and study the absorption of polaritons by measuring the Brillouin oscillations, which result from the interaction of the polaritons with the picosecond strain pulse. Based on the earlier experimental studies of polaritons in MQWs we perform modeling of polariton dynamics and show the decisive role of exciton phase transition in the experimentally observed transparency effect. The studied phenomenon complements the family of optically induced transparency effects. It has features common with saturable absorption,[1,5,41] but in our case, the full transparency involves the transition into a noncoherent exciton gas instead of equalizing the population of the ground and excited states. Studying optically induced transparency by TDBS is prospective for understanding the excitation density and optical field inside the nanostructures. To that end, a comprehensive theoretical model should be developed to provide the comparison of the measured and simulated signals on a quantitative level. Currently, such comparison in nanophotonic devices has been done only for low densities in the linear excitation regime.[17] From the experimental point of view, the spatial resolution may be improved by using spatially shorter strain pulses[42] and higher frequencies of the TDBS oscillations.[43]

METHODS

Sample Fabrication. The studied structure was grown by molecular beam epitaxy on top of a 100 nm GaAs buffer and a semi-insulating (100) GaAs substrate. The structure consists of 30 pairs of GaAs/$Ga_{0.67}Al_{0.33}As$ with thicknesses of 17.5/8 nm. The top layer is covered by a single 8 nm layer of $Ga_{0.67}Al_{0.33}As$ and finally with a 5 nm layer of GaAs. The total thickness of the polaritonic layer is L = 778 nm. For the experiments, the substrate was polished down to 105 μm thickness, and an Al film of 100 nm thickness was deposited on its backside by magnetron sputtering for the generation of picosecond strain pulses. The sample was mounted on a metallic coldfinger in the vacuum chamber of a flow Helium cryostat.

Optical Excitation of Polaritons in MQWs. The laser source for the excitation of polaritons is a tunable Ti/sapphire laser oscillator with 76 MHz pulse repetition rate and 120 fs pulse duration. The photon energy is tuned around the spectral position of the polariton resonance, $\hbar\omega$ = 1.5307 eV (wavelength λ = 810 nm). The laser beam is retarded by a fixed mechanical delay line by 20 ns (traveling time of the strain pulse through the GaAs substrate) and passed through a tunable double liquid crystal filter (VariSpec) with a transmission band of 0.8 nm spectral width centered at the laser photon energy. The laser beam is focused on the front surface of the MQW layer to a spot of 40 μm diameter, opposite to the spot on the Al film emitting the strain pulse. The intensity of the reflected from the sample light was measured by a Si-photoreceiver with 500 kHz bandwidth. The TDBS signal is measured with a 100 MHz lock-in amplifier synchronized with a mechanical chopper, which interrupts the laser beam exciting the Al film at the frequency of 5.5 kHz. The time delay, t, is controlled by a 10 cm multipass mechanical delay line. The steady-state parameters of the polariton resonance, E_0, E_{LT} and Γ_0, were obtained from a reflectivity spectrum measured using a halogen lamp and a 0.5 m single monochromator with a CCD-camera.

Picosecond Strain Pulses. The strain pulses are generated as a result of pulsed optical excitation of the Al film by the same femtosecond laser which is used for excitation of the polaritons in the MQWs. The Al film expands and the picosecond strain pulse is injected into the GaAs substrate. The temporal/spatial shape of the strain pulse is calculated based on a two-temperature model[44] and was confirmed by direct measurements in earlier works.[29] However, at low temperature ($T \sim 10$ K) the diffusion of hot electrons plays an important role for the spatial shape of the generated strain pulse. This process depends on the polycrystalline properties of the deposited Al film which cannot be estimated precisely. This gives some uncertainty in the amplitude and spatial shape of the strain pulses. This uncertainty gives the factor of 2 difference in the calculated and measured amplitudes of the TDBS signals.

SIMULATIONS

The dependence $\Gamma(N)$ is given by the phenomenological eq 4 (see also inset in Figure 2c), where the function $\mathcal{R}$ describes the phase transition of the exciton gas and may be modeled as

$$\mathcal{R}(N) = B[1 + e^{N_t - N/\Delta N}]^{-1} \tag{6}$$

where the threshold exciton density N_t and the width of the phase transition ΔN are given in the main text. The coefficient B should be taken much larger than βN_t. In the calculations we use B = 0.3 eV.

In the simulations the temporal and spatial intervals are divided into small steps with the widths $d\tau$ and dx, respectively. Then the changes dN of incoherent excitons generated from the polaritons during time $d\tau$ may be written as

$$dN(x, \tau) = \frac{I(x, \tau)\alpha(x, \tau)}{eE} d\tau \tag{7}$$

where the absorption coefficient

$$\alpha(x, \tau) = \frac{2\pi}{n\lambda} \frac{\varepsilon_b E_{LT} \Gamma(x, \tau)}{(E_0 - E)^2 + \Gamma(x, \tau)^2} \tag{8}$$

and $I(x,\tau)$ is the polariton intensity flux at time τ and distance x. Near the surface, x = 0

$$I(\tau) = (1 - R_0)\sqrt{\frac{2}{\pi}}\left(\frac{J}{\tau_e}\right) e^{-2\left(\frac{\tau}{\tau_e}\right)^2} \tag{9}$$

Substituting eqs 8 and 9 into 7 and solving numerically the differential equation eq 7, we find $N(x = 0,\tau)$ with the initial condition $N = 0$ at $\tau \to -\infty$. Further we calculate $I(x,\tau)$ for the next position $x + dx$ as $I(x + dx,\tau) = I(x,\tau)e^{-\alpha(x,\tau)dx}$ and again use eq 7 to calculate $N(x + dx,\tau)$. Repeating this cycle, we finally calculate $N(x,\tau)$ for all τ and x. We have checked that the variation of N does not change significantly the reflected intensity R_0.

To calculate the TDBS signal we use the transfer matrix formalism and calculate the intensity of the reflected light as a function of time τ with variable $\Gamma(x,\tau)$ in the presence of the strain pulse. Then we calculate the integrated reflected intensity across the full excitation pulse duration. Finally, we plot the intensity reflectivity changes as a function of the delay time t between the excitation and strain pulses.

https://doi.org/10.1021/acsphotonics.4c01357
ACS Photonics XXXX, XXX, XXX−XXX

■ ASSOCIATED CONTENT

Supporting Information

The Supporting Information is available free of charge at https://pubs.acs.org/doi/10.1021/acsphotonics.4c01357.

(1) Calculations of exciton density; (2) the shape of strain pulse; (3) simulation of TDBS signal; (4) dependences on parameters of Γ in eq 4; (5) inhomogeneous broadening of the exciton resonance (PDF)

■ AUTHOR INFORMATION

Corresponding Authors

Alexey V. Scherbakov − *Experimentelle Physik 2, Technische Universität Dortmund, 44227 Dortmund, Germany;* orcid.org/0000-0001-7358-4164; Email: alexey.shcherbakov@tu-dortmund.de

Andrey V. Akimov − *School of Physics and Astronomy, University of Nottingham, NG7 2RD Nottingham, U.K.;* orcid.org/0000-0002-8173-8212; Email: andrey.akimov@nottingham.ac.uk

Authors

Marek Karzel − *Experimentelle Physik 2, Technische Universität Dortmund, 44227 Dortmund, Germany*

Anton K. Samusev − *Experimentelle Physik 2, Technische Universität Dortmund, 44227 Dortmund, Germany;* orcid.org/0000-0002-3547-6573

Tetiana L. Linnik − *Experimentelle Physik 2, Technische Universität Dortmund, 44227 Dortmund, Germany; Department of Theoretical Physics, V. E. Lashkaryov Institute of Semiconductor Physics, 03028 Kyiv, Ukraine*

Mario Littmann − *Department Physik, Universität Paderborn, 33098 Paderborn, Germany;* orcid.org/0000-0003-0875-3720

Dirk Reuter − *Department Physik, Universität Paderborn, 33098 Paderborn, Germany*

Manfred Bayer − *Experimentelle Physik 2, Technische Universität Dortmund, 44227 Dortmund, Germany;* orcid.org/0000-0002-0893-5949

Complete contact information is available at: https://pubs.acs.org/10.1021/acsphotonics.4c01357

Author Contributions

A.V.S. designed and directed the project. M.K. and A.K.S. carried out the experimental studies and analyzed the experimental data. T.L.L. and A.V.A. performed the theoretical modeling. M.L. and D.R. designed and fabricated the polaritonic structure. M.B. developed the concept and supervised the research program. A.V.A. wrote the first draft of the manuscript. A.V.S. designed the experiment and supervised the overall research. A.K.S., T.L.L., A.V.A., and A.V.S. wrote the manuscript. All authors discussed the experimental and numerical results and edited the manuscript.

Funding

The work was funded by the Deutsche Forschungsgemeinschaft (SFB-Geschäftszeichen TRR142/3-2022-Projektnummer 231447078, Projects A06 and B08) and the research center "Future Energy Materials and Systems" of the Research Alliance Ruhr. A.K.S. acknowledges the support of the Deutsche Forschungsgemeinschaft through the Walter Benjamin Programme (project #529710370). T.L.L. acknowledges the Alexander von Humboldt Foundation support through the Philipp Schwartz Initiative and TU Dortmund core funds. A.V.S. acknowledges the Mercur Foundation (Grant Pe-2019-0022). A.V.A. acknowledges the Alexander von Humboldt Foundation.

Notes

The authors declare no competing financial interest.

■ REFERENCES

(1) Allen, A.; Eberly, J. H. *Optical Resonance and Two-Level Atoms*; Wiley: New York, 1975.

(2) Fleischhauer, M.; Imamoğlu, A.; Marangos, J. P. Electromagnetically induced transparency: optics in coherent media. *Rev. Mod. Phys.* **2005**, *77*, 633−673.

(3) McCall, S. L.; Hahn, E. L. Self-induced transparency. *Phys. Rev.* **1969**, *183*, 457−485.

(4) Giessen, H.; Knorr, A.; Haas, S.; Koch, S. W.; Linden, S.; Kuhl, J.; Hetterich, M.; Grün, M.; Klingshirn, C. Self-induced transmission on a free exciton resonance in a semiconductor. *Phys. Rev. Lett.* **1998**, *81*, 4260−4263.

(5) Frantz, L. M.; Nodvik, J. S. Theory of Pulse Propagation in a Laser Amplifier. *J. Appl. Phys.* **1963**, *34*, 2346−2349.

(6) Clementi, M.; Iadanza, S.; Schulz, S. A.; Urbinati, G.; Gerace, D.; O'Faloain, L.; Galli, M. Thermo-optically induced transparency on a photonic chip. *Light: Sci. Appl.* **2021**, *10*, 240.

(7) Qin, H. Y.; Ding, M.; Yin, Y. H. Induced Transparency with Optical Cavities. *Adv. Photonics Res.* **2020**, *1*, 2000009.

(8) Zhu, S.; Wang, W. Y.; Ren, L. H.; Gong, C. Y.; Chen, Y. C.; Shi, L.; Zhang, X. L. Thermal gradient induced transparency and absorption in a microcavity. *Laser Photonics Rev.* **2023**, *17*, 2200644.

(9) Brabec, T.; Krausz, F. Intense few-cycle laser fields: Frontiers of nonlinear optics. *Rev. Mod. Phys.* **2000**, *72*, 545−591.

(10) Watanabe, K.; Nakano, H.; Honold, A.; Yamamoto, Y. Optical nonlinearities of excitonic self-induced-transparency solitons: Toward ultimate realization of squeezed states and quantum nondemolition measurement. *Phys. Rev. Lett.* **1989**, *62*, 2257−2260.

(11) Hau, L. V.; Harris, S. E.; Dutton, Z.; Behroozi, C. H. Light speed reduction to 17 metres per second in an ultracold atomic gas. *Nature* **1999**, *397*, 594−598.

(12) Longdell, J. J.; Fraval, E.; Sellars, M. J.; Manson, N. B. Stopped light with storage times greater than one second using electromagnetically induced transparency in a solid. *Phys. Rev. Lett.* **2005**, *95*, 063601.

(13) Bigelow, M. S.; Lepeshkin, N. N.; Boyd, R. W. Superluminal and slow light propagation in a room temperature solid. *Science* **2003**, *301*, 200−202.

(14) Thomsen, C.; Grahn, H. T.; Maris, H. J.; Tauc, J. Picosecond interferometric technique for study of phonons in the brillouin frequency range. *Opt. Commun.* **1986**, *60*, 55−58.

(15) Lin, H. N.; Stoner, R. J.; Maris, H. J.; Tauc, J. Phonon attenuation and velocity measurements in transparent materials by picosecond acoustic interferometry. *J. Appl. Phys.* **1991**, *69*, 3816−3822.

(16) Matsuda, O.; Larciprete, M. C.; Li Voti, R.; Wright, O. B. Fundamentals of picosecond laser ultrasonics. *Ultrasonics* **2015**, *56*, 3−20.

(17) Kobecki, M.; Scherbakov, A. V.; Kukhtaruk, S. M.; Yaremkevich, D. D.; Henksmeier, T.; Trapp, A.; Reuter, D.; Gusev, V. E.; Akimov, A. V.; Bayer, M. Giant photoelasticity of polaritons for detection of coherent phonons in a superlattice with quantum sensitivity. *Phys. Rev. Lett.* **2022**, *128*, 157401.

(18) Mechri, C.; Ruello, P.; Breteau, J. M.; Baklanov, M. R.; Verdonck, P.; Gusev, V. Depth-profiling of elastic inhomogeneities in transparent nanoporous low-k materials by picosecond ultrasonic interferometry. *Appl. Phys. Lett.* **2009**, *95*, 091907.

(19) Hudert, F.; Bartels, A.; Dekorsy, T.; Köhler, K. Influence of doping profiles on coherent acoustic phonon detection and generation in semiconductors. *J. Appl. Phys.* **2008**, *104*, 123509.

(20) Gusev, V. E.; Thréard, T.; Hurley, D. H.; Raetz, S. Time-domain Brillouin scattering theory for probe light and acoustic beams propagating at an angle and acousto-optic interaction at material interfaces. *Photoacoustics* **2023**, *33*, 100563.
(21) Shen, C. C.; Weng, M. Y.; Sheu, J. K.; Yao, Y. T.; Sun, C. K. In Situ Monitoring of Chemical Reactions at a Solid−Water Interface by Femtosecond Acoustics. *J. Phys. Chem. Lett.* **2017**, *8*, 5430−5437.
(22) Czerniuk, T.; Schneider, C.; Kamp, M.; Höfling, S.; Glavin, B. A.; Yakovlev, D. R.; Akimov, A. V.; Bayer, M. Acousto-optical nanoscopy of buried photonic nanostructures. *Optica* **2017**, *4*, 588−594.
(23) Ivchenko, E. L. *Optical Spectroscopy of Semiconductor Nanostructures*; Springer: Berlin, Heidelberg, New York, Hong Kong, London, Milan, Paris, Tokyo, 2004.
(24) Kosobukin, V. A. Transmission and reflection of light by semiconductor superlattices in the region of excitonic resonances. *Sov. Phys. Solid State* **1992**, *34*, 1662−1668.
(25) Hopfield, J. J. Theory of the contribution of excitons to complex dielectric constant of crystals. *Phys. Rev.* **1958**, *112*, 1555−1567.
(26) Jusserand, B.; Fainstein, A.; Ferreira, R.; Majrab, S.; Lemaitre, A. Dispersion and damping of multiple quantum-well polaritons from resonant Brillouin scattering by folded acoustic modes. *Phys. Rev. B:Condens. Matter Mater. Phys.* **2012**, *85*, 041302.
(27) Jusserand, B.; Poddubny, A. N.; Poshakinskiy, A. V.; Fainstein, A.; Lemaitre, A. Polariton resonances for ultrastrong coupling cavity optomechanics in GaAs/AlAs Multiple Quantum Wells. *Phys. Rev. Lett.* **2015**, *115*, 267402.
(28) Poddubny, A. N.; Poshakinskiy, A. V.; Jusserand, B.; Lemaître, A. Resonant Brillouin scattering of excitonic polaritons in multiple-quantum-well structures. *Phys. Rev. B:Condens. Matter Mater. Phys.* **2014**, *89*, 235313.
(29) Scherbakov, A. V.; van Capel, P. J. S.; Akimov, A. V.; Dijkhuis, J. I.; Yakovlev, D. R.; Berstermann, T.; Bayer, M. Chirping of an optical transition by an ultrafast acoustic soliton train in a semiconductor quantum well. *Phys. Rev. Lett.* **2007**, *99*, 057402.
(30) Thomsen, C.; Grahn, H. T.; Maris, H. J.; Tauc, J. Surface generation and detection of phonons by picosecond light pulses. *Phys. Rev. B:Condens. Matter Mater. Phys.* **1986**, *34*, 4129−4138.
(31) Pollak, F. H.; Cardona, M. Piezo-Electroreflectance in Ge, GaAs, and Si. *Phys. Rev.* **1968**, *172*, 816−837.
(32) Jahnke, F.; Koch, M.; Meier, T.; Feldmann, J.; Schafer, W.; Thomas, P.; Koch, S. W.; Gobel, E. O.; Nickel, H. Simultaneous influence of disorder and Coulomb interaction on photon echoes in semiconductors. *Phys. Rev. B:Condens. Matter Mater. Phys.* **1994**, *50*, 8114−8117.
(33) Feldmann, J.; Peter, G.; Gobel, E. O.; Dawson, P.; Moore, K.; Foxon, C.; Elliott, J. Linewidth Dependence of Radiative Exciton Lifetimes in Quantum Wells. *Phys. Rev. Lett.* **1987**, *59*, 2337−2340.
(34) Eccleston, R.; Feuerbacher, B. F.; Kuhl, J.; Rühle, W. W.; Ploog, K. Density-dependent exciton radiative lifetimes in GaAs quantum wells. *Phys. Rev. B:Condens. Matter Mater. Phys.* **1992**, *45*, 11403−11406.
(35) Honold, A.; Schultheis, L.; Kuhl, J.; Tu, C. W. Collision broadening of two-dimensional excitons in a GaAs single quantum well. *Phys. Rev. B:Condens. Matter Mater. Phys.* **1989**, *40*, 6442−6445.
(36) Manzke, G.; Semkat, D.; Stolz, H. Mott transition of excitons in GaAs-GaAlAs quantum wells. *New J. Phys.* **2012**, *14*, 095002.
(37) Manzke, G.; Richter, F.; Semkat, D.; Burau, G. K. G.; Kieseling, F.; Stolz, H. Transition from excitonic to plasma emission from localized electron-hole pair states in GaAs-AlGaAs quantum wells. *Phys. Status Solidi C* **2011**, *8*, 1161−1164.
(38) Fehrenbach, G. W.; Schafer, W.; Treusch, J.; Ulbrich, R. G. Transient Optical Spectra of a Dense Exciton Gas in a Direct-Gap Semiconductor. *Phys. Rev. Lett.* **1982**, *49*, 1281−1284.
(39) Huber, R.; Kaindl, R. A.; Schmid, B. A.; Chemla, D. S. Broadband terahertz study of excitonic resonances in the high-density regime in GaAs/$Al_xGa_{1-x}As$ quantum wells. *Phys. Rev. B:Condens. Matter Mater. Phys.* **2005**, *72*, 161314.
(40) Burau, G. K. G.; Manzke, G.; Kieseling, F.; Stolz, H.; Reuter, D.; Wieck, A. Nonlinear behaviour of the resonance fluorescence from excitons in quantum wells. *J. Phys.: Conf. Ser.* **2010**, *210*, 012017.
(41) Wang, G. Z.; Baker-Murray, A. A.; Blau, W. J. Saturable Absorption in 2D Nanomaterials and Related Photonic Devices. *Laser Photonics Rev.* **2019**, *13*, 1800282.
(42) Yoon, Y.; Lu, Z.; Uzundal, C.; Qi, R.; Zhao, W.; Chen, S.; Feng, Q.; Kim, W.; Naik, M. H.; Watanabe, K.; Taniguchi, T.; Louie, S. G.; Crommie, M. F.; Wang, F. Terahertz phonon engineering with van der Waals heterostructures. *Nature* **2024**, *631*, 771−776.
(43) van Capel, P. J. S.; Turchinovich, D.; Porte, H. P.; Lahmann, S.; Rossow, U.; Hangleiter, A.; Dijkhuis, J. I. Correlated terahertz acoustic and electromagnetic emission in dynamically screened InGaN/GaN quantum wells. *Phys. Rev. B:Condens. Matter Mater. Phys.* **2011**, *84*, 085317.
(44) Wright, O. B.; Gusev, V. E. Ultrafast generation of acoustic waves in copper. *IEEE Trans. Sonics Ultrason.* **1995**, *42*, 331−338.

https://doi.org/10.1021/acsphotonics.4c01357
ACS Photonics XXXX, XXX, XXX−XXX